Initial Characterization of Geopolymer-Based UHPC Material Properties

Final Report
August 2018

Sponsored by
Iowa Highway Research Board
(IHRB Project TR-708A)
Midwest Transportation Center
U.S. DOT Office of the Assistant Secretary
for Research and Technology

MIDWEST TRANSPORTATION CENTER
MTC
IOWA STATE UNIVERSITY
Institute for Transportation

About MTC

The Midwest Transportation Center (MTC) is a regional University Transportation Center (UTC) sponsored by the U.S. Department of Transportation Office of the Assistant Secretary for Research and Technology (USDOT/OST-R). The mission of the UTC program is to advance U.S. technology and expertise in the many disciplines comprising transportation through the mechanisms of education, research, and technology transfer at university-based centers of excellence. Iowa State University, through its Institute for Transportation (InTrans), is the MTC lead institution.

About InTrans

The mission of the Institute for Transportation (InTrans) at Iowa State University is to develop and implement innovative methods, materials, and technologies for improving transportation efficiency, safety, reliability, and sustainability while improving the learning environment of students, faculty, and staff in transportation-related fields.

ISU Non-Discrimination Statement

Iowa State University does not discriminate on the basis of race, color, age, ethnicity, religion, national origin, pregnancy, sexual orientation, gender identity, genetic information, sex, marital status, disability, or status as a U.S. veteran. Inquiries regarding non-discrimination policies may be directed to Office of Equal Opportunity, 3410 Beardshear Hall, 515 Morrill Road, Ames, Iowa 50011, Tel. 515-294-7612, Hotline: 515-294-1222, email eooffice@iastate.edu.

Notice

The contents of this report reflect the views of the authors, who are responsible for the facts and the accuracy of the information presented herein. The opinions, findings and conclusions expressed in this publication are those of the authors and not necessarily those of the sponsors.

This document is disseminated under the sponsorship of the U.S. DOT UTC program in the interest of information exchange. The U.S. Government assumes no liability for the use of the information contained in this document. This report does not constitute a standard, specification, or regulation.

The U.S. Government does not endorse products or manufacturers. If trademarks or manufacturers' names appear in this report, it is only because they are considered essential to the objective of the document.

Quality Assurance Statement

The Federal Highway Administration (FHWA) provides high-quality information to serve Government, industry, and the public in a manner that promotes public understanding. Standards and policies are used to ensure and maximize the quality, objectivity, utility, and integrity of its information. The FHWA periodically reviews quality issues and adjusts its programs and processes to ensure continuous quality improvement.

Iowa DOT Statements

Federal and state laws prohibit employment and/or public accommodation discrimination on the basis of age, color, creed, disability, gender identity, national origin, pregnancy, race, religion, sex, sexual orientation or veteran's status. If you believe you have been discriminated against, please contact the Iowa Civil Rights Commission at 800-457-4416 or the Iowa Department of Transportation affirmative action officer. If you need accommodations because of a disability to access the Iowa Department of Transportation's services, contact the agency's affirmative action officer at 800-262-0003.

Technical Report Documentation Page

1. Report No. IHRB Project TR-708A	**2. Government Accession No.**	**3. Recipient's Catalog No.**	
4. Title and Subtitle Initial Characterization of Geopolymer-Based UHPC Material Properties		**5. Report Date** August 2018 **6. Performing Organization Code**	
7. Author(s) Jay Shen (orcid.org/0000-0002-8201-5569), Ping Lu (orcid.org/0000-0002-9427-2415), Yifeng Ling (orcid.org/0000-0002-8846-0524), and Mahmoud Faytarouni (orcid.org/0000-0003-4231-158X)		**8. Performing Organization Report No.**	
9. Performing Organization Name and Address Institute for Transportation Iowa State University 2711 South Loop Drive, Suite 4700 Ames, IA 50010-8664		**10. Work Unit No. (TRAIS)** **11. Contract or Grant No.** Part of DTRT13-G-UTC37	
12. Sponsoring Organization Name and Address Midwest Transportation Center 2711 S. Loop Drive, Suite 4700 Ames, IA 50010-8664 Iowa Highway Research Board Iowa Department of Transportation 800 Lincoln Way Ames, Iowa	U.S. Department of Transportation Office of the Assistant Secretary for Research and Technology 1200 New Jersey Avenue, SE Washington, DC 20590	**13. Type of Report and Period Covered** Final Report **14. Sponsoring Agency Code**	
15. Supplementary Notes Visit www.intrans.iastate.edu for color pdfs of this and other research reports.			

16. Abstract

Ultra-high-performance concrete (UHPC) has great potential as a structural material for bridge engineering due to its excellent strength, ductility, and durability. However, the high Portland cement content required by conventional UHPC poses a major obstacle to widespread practical application because of its high cost and CO_2 emissions. Introducing any sort of composites as replacements for Portland cement would have a positive impact on the practical applications of UHPC. This research project investigated the mechanical properties (such as compression, tension, bending strength, and modulus of elasticity) of geopolymer-based UHPC and a type of composite UHPC using Iowa materials to explore the feasibility of their use in UHPC for transportation infrastructure.

In this study, different ultra-high-performance geopolymer (UHPG) mixes were formulated, their mechanical properties were evaluated, and effects of curing methods on the UHPG strength were investigated. The results indicated that usable UHPG can be achieved through engineered formulation using locally available concrete materials. The UHPG sample made in China and tested at Iowa State University (ISU) showed a compressive strength of 123 MPa (17,868 psi) and maximum compressive strain of 0.0047 micro-strain. The UHPG samples made with a slag-fly ash blend and a liquid (activator solution)-to-binder (slag and fly ash) of 0.27 had 28-day compressive strength of 102 MPa (14,800 psi). When reinforced with 2% (by volume) of polyvinyl alcohol (PVA) fiber, the UHPG mixes developed at ISU exhibited strain and displacement hardening behavior in tension and flexure, indicating significant ductility. Replacement of slag for fly ash improved strengths and elastic modulus, but noticeably reduced the deflection at failure and ductility of UHPG. Steam curing at 50°C appeared to be the optimal condition for the UHPG strength development.

17. Key Words ductility—geopolymer-based UHPC—slag replacement—ultra-high-performance concrete—ultra-high strength		**18. Distribution Statement** No restrictions.	
19. Security Classification (of this report) Unclassified.	**20. Security Classification (of this page)** Unclassified.	**21. No. of Pages** 42	**22. Price** NA

Form DOT F 1700.7 (8-72) **Reproduction of completed page authorized**

Initial Characterization of Geopolymer-Based UHPC Material Properties

Final Report
August 2018

Principal Investigator
Jay Shen, Associate Professor
Civil, Construction, and Environmental Engineering
Iowa State University

Co-Principal Investigator
Ping Lu, Preservation Engineer
Office of Bridges and Structures
Iowa Department of Transportation

Research Assistants
Yifeng Ling and Mahmoud Faytarouni

Authors
Jay Shen, Ping Lu, Yifeng Ling, and Mahmoud Faytarouni

Sponsored by
Midwest Transportation Center,
U.S. Department of Transportation
Office of the Assistant Secretary for Research and Technology,
Iowa Department of Transportation, and
Iowa Highway Research Board
(IHRB Project TR-708A)

Preparation of this report was financed in part
through funds provided by the Iowa Department of Transportation
through its Research Management Agreement with the
Institute for Transportation

A report from
Institute for Transportation
Iowa State University
2711 South Loop Drive, Suite 4700
Ames, IA 50010-8664
Phone: 515-294-8103 / Fax: 515-294-0467
www.intrans.iastate.edu

TABLE OF CONTENTS

LIST OF FIGURES

LIST OF TABLES

ACKNOWLEDGEMENTS

The authors would like to thank the Iowa Department of Transportation (DOT), Iowa Highway Research Board (IHRB), Midwest Transportation Center, and U.S. Department of Transportation Office of the Assistant Secretary for Research and Technology for sponsoring this project. This was one of four pilot projects for novel or innovative ideas and fundamental advances that were sponsored.

EXECUTIVE SUMMARY

Ultra-high-performance concrete (UHPC) has attracted much interest in the bridge engineering community over the past decades due to its excellent strength, ductility, and durability. However, the high cement content required by conventional UHPC has made it expensive and less environmental friendly due to the CO_2 emissions resulting from cement manufacture.

Recently, a unique, innovative, and low-cost geopolymer-based UHPC, also called ultra-high-performance geopolymer (UHPG), has been developed in China, where geopolymer composites are used to replace Portland cement in conventional UHPC. With geopolymer as a binder, UHPG is not only cost effective but also environmentally friendly. The UHPG in China was originally developed for applications in protective structures, and research conducted so far has mainly focused on its blast-resistant properties.

This research project was originally designed to evaluate the properties of the UHPG made in China and to explore the feasibility of its use for transportation infrastructure. However, due to difficulties in obtaining UHPG samples from China, the project was expanded to consider the development of UHPG using Iowa materials. In addition to formulating UHPG mix proportions, the mechanical properties (such as compression, tension, bending strength, and modulus of elasticity) of the newly developed UHPG were evaluated according to ASTM International and/or American Association of State Highway Transportation Officials (AASHTO) test methods. The effects of curing condition on the UHPG strength development were also investigated.

The following conclusions were drawn from this work:

- The UHPG sample made in China and tested at Iowa State University (ISU) showed a compressive strength of 123 MPa (17,868 psi) and maximum compressive strain of 0.0047 microstrains.

- The mix design study at ISU revealed that the compressive strength of fly ash based UHPG could be enhanced by replacing fly ash with ground-granulated blast-furnace slag (GGBFS or slag). However, the optimal slag content was 20%. The UHPG samples made with 20% slag replacement for fly ash and a liquid (activator solution)-to-binder (slag and fly ash) of 0.27 had a 28-day compressive strength of 102 MPa (14,800 psi), about 20% lower than that of the UHPG sample made in China.

- When reinforced with 2% (by volume) of polyvinyl alcohol (PVA) fiber, the UHPG mixes developed at ISU (with 0-30% slag replacement for fly ash) exhibited strain and displacement hardening behavior in tension and flexure, indicating significant ductility.

- Use of slag as a replacement for fly ash improved the strengths and elastic modulus of UHPG but noticeably reduced the deflection at failure and ductility of UHPG.

- As slag content increased, the bond strength between the geopolymer and steel rebar

improved. The UHPG samples with 20% slag replacement showed a 77.1% increase in bond strength when compared with that of pure fly ash UHPG.

- Among the curing methods used, steam curing at 50°C appeared to be the best condition for UHPG strength development.

The following recommendations are proposed based on the project observations and conclusions:

- Due to the short period of time for this study, only a limited number of UHPG mixes were studied in this project. The ISU UHPG achieved very good strength (102 MPa or 14,800 psi) but it was still lower than that of the sample from China. Further studies should be done to increase the density and reduce the porosity of the ISU UHPG.

- The UHPG samples made at ISU were cured at an elevated temperature (50ºC). In consideration of field use, ambient temperature curing for the strength development of UHPG should be studied in order to reduce the cost.

- The present study focused on the mechanical properties of UHPG only. Although geopolymers were reported to have excellent chemical resistance, the durability properties of UHPG, such as freezing and thawing resistance, should be studied for its potential use in Iowa.

1. INTRODUCTION

1.1 Problem Statement

Ultra-high-performance concrete (UHPC) has been attracting more and more interest in the bridge engineering community due to its excellent strength, ductility, and durability. These characteristics can lead to the construction of a much lighter bridge structure and lower associated maintenance costs. The Iowa Department of Transportation (DOT) is a leading state agency in UHPC research and application. Multiple projects using UHPC have been successfully completed during the past 15 years, and the advantages were widely observed. However, the biggest hurdle for wider adoption of UHPC in civil construction projects is its extremely high material cost. The cost of Ductal UHPC—the most dominant and only commercially available UHPC product in the US—is about 10 to 20 times higher than the cost of regular concrete. Additionally, the cost of Korean UHPC (K-UHPC), a lower cost alternative to Ductal UHPC, is about 3 to 5 times as high. Finding a cost-effective UHPC material is essential to expanding the future engineering applications of UHPC.

Recently, Chinese researchers successfully developed a low-cost UHPC formulation–a geopolymer based UHPC, or UHPG, that is only 50% more expensive than conventional concrete. The results of the material testing of UHPG conducted by Australian and Chinese research teams showed that its properties are comparable to Ductal UHPC. The lower cost and improved performance of the new formula are achieved mainly by replacing the cement found in traditional UHPC with geopolymer materials. The material's performance is further improved by using a nano-scale additive to fill voids and enhance the hydration process. The use of geopolymer materials makes the product both cost effective and environmentally friendly. This UHPG formula is unique, innovative, and shows much promise. No similar product is commercially available in the US. UHPG was originally developed for applications in protective structures and research conducted so far has mainly focused on its blast resistance properties. The present research was intended to evaluate the properties of the UHPG made in China and to explore the feasibility of its use for transportation infrastructure.

Because it was very difficult to obtain (transport) UHPG samples from China, the project was expanded to study the development of UHPG using Iowa materials. In addition to formulating UHPG mix proportions, the mechanical properties (such as compression, tension, bending strength, and modulus of elasticity) of the newly developed UHPG were evaluated according to ASTM International and/or American Association of State Highway Transportation Officials (AASHTO) test methods. The effects of curing conditions on UHPG strength development were investigated.

It is expected that in the future, the design concept will be laboratory tested and a cost-benefit study carried out to compare the cost of the UHPG design with traditional design. With the reduced material cost and higher performance of the UHPG, it is very possible that the initial construction cost of a bridge made with UHPG will be comparable to or only slightly higher than that of a traditional bridge. If the reduced long-term maintenance costs are included, the cost/benefit ratio of using UHPG would be easily justified. It is also anticipated that after

successful evaluation of the important material properties, the cost-effective and environmentally friendly qualities of UHPG may make it a very attractive option for future bridge construction and repair. If successful, this work would lead to a reduction in the overall bridge life-cycle cost by taking advantage of the higher strength and the very low (close to zero) permeability which could essentially eliminate deterioration. When budgets are severely limited, being able to reduce maintenance costs is essential for sustaining a state of good repair.

1.2 Scope of Study

This study carried out three main tasks:

1. Conduct a literature review on the approaches and methods for all laboratory tests

2. Characterize the mechanical properties of UHPG including compressive, tensile strength, bending flexural strength, and bond strength

3. Analyze all test results and develop the final project report

2. LITERATURE REVIEW

2.1 Background of Geopolymer

Demands to reduce the use of Portland cement (PC) in concrete have been rising along with awareness of the increasing environmental issues caused by CO_2 from production of PC. These concerns have accelerated the development of a geopolymer binder that was a product from the reaction of industrial aluminosilicate wastes (e.g., fly ash, slag, and metakaolin) and alkali solution (Sumajouw et al. 2004). As a new type of concrete binder, geopolymer has been recognized as an alternative to traditional PC due to its high temperature, acid resistance, and environmental benefits (e.g., significant reduction of CO_2 emissions). Since Joseph Davidovits coined the term "geopolymer" in 1978, its properties and uses have been explored by many scientific and industrial researchers (Davidovits 1994).

Geopolymers are characterized by a three-dimensional Si-O-Al structure and are able to provide ceramic and zeolitic properties that are not normally present in PC (McDonald and Thompson n.d.). Geopolymer develops through several distinct reaction processes from initial pozzolanic activation to final microstructure development (Fernández-Jiménez et al. 2005). The major steps in geopolymer formation are as follows:

1. Dissolution of the aluminosilicate species within a highly alkaline environment

2. Polymerization of the dissolved ions into temporary structural gel

3. Precipitation of formed hydration products

4. Final hardening of the matrix by excess water evaporation

5. Growth of crystalline structures

Figure 2.1 illustrates the overall polymerization process in geopolymer, which can be summarized as a three-step process: dissolution, polymerization, and growth (Rangan 2008).

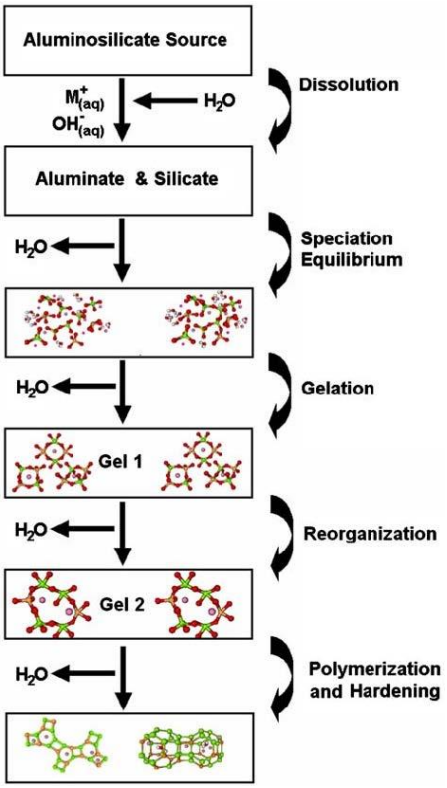

Duxson et al. 2007, © Springer Science+Business Media, LLC 2006

Figure 2.1. Geopolymer development model

Dissolution occurs immediately after the contact of the alkaline solution and the pozzolanic materials and creates an ionic interface that facilitates the breaking of covalent bonds among silicon, aluminum, and oxygen atoms. Similar to PC, this process generates rapid and intense heat (Fernández-Jiménez et al. 2006a). The rate of dissolution correlates to the amount and composition of the activating solution (Xie and Xi 2001). The polymerization process involves a rapid chemical reaction in an alkaline solution on Si-Al species, resulting in a three-dimensional polymeric chain-and-ring structure consisting of Si-O-Al-O bonds (Skvara et al. 2006). The formed gel contains alkaline cations that compensate for the charge deficit associated with the Al-for-Si substitution (Xie and Xi 2001). An intermediate, Al-rich phase forms first, and gives way to a more stable, silicon-rich, three-dimensional gel that is dependent upon curing conditions and activator type (Fernández-Jiménez et al. 2006b). During this process, the slow growth of crystalline structures becomes evident as the nuclei of the polymerized gel reach critical size. The degree of crystallinity relates to the rate at which precipitation occurs. It should be noted that the fast reactions between alkali and pozzolanic materials do not allow enough time for the growth of a well-structured crystalline environment. Therefore, most hardened geopolymers are referred to as zeolitic precursors rather than actual zeolites. The final product of geopolymerization is an amorphous, semi-crystalline cementitious material (Petermann et al. 2010).

2.2 Commonly Used Aluminosilicate Materials

As mentioned previously, the major geopolymer materials are usually industrial wastes containing aluminosilicate, such as fly ash, slag, metakaolin, etc. The most commonly used aluminosilicate precursor in one-part geopolymer mixes is fly ash. Research has also shown that a partial slag replacement for fly ash could help strength development of fly ash-based geopolymers. In this study, fly ash was used as a major precursor, and slag was used as a partial replacement in geopolymer synthetization.

The most readily available pozzolanic material around the world is fly ash, which is a by-product obtained from the combustion of coal during industrial processes like power generation. It is considered one of the most important source materials for geopolymer binder (Khale and Chaudhary 2007). Most fly ashes from the combustion of coal are made up of an inhomogeneous mix of aluminosilicate and silica glasses, plus small amounts of crystalline materials including mullite, quartz, hematite, and magnetite (Song et al. 2000). Particle size distribution and fineness (see Figure 2.2) are the physical characteristics of fly ashes most strongly governing their reactivity.

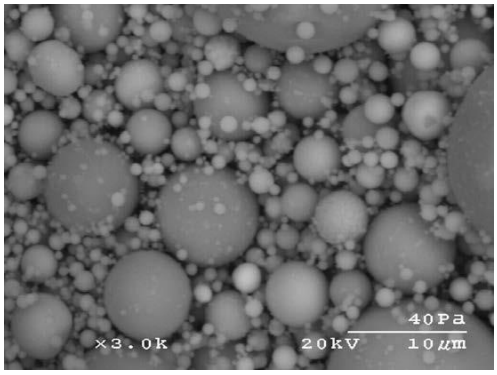

Wang and Ge 2003

Figure 2.2. Microscopic image of raw fly ash

The presence of highly reactive silica in the fly ash increases the formation potential of aluminosilicate gel, which contributes mechanical strength to the geopolymer. The aluminum content of fly ash material is critical to the hardening properties of a geopolymer binder and is believed to be the critical factor for setting (Rangan 2008).

2.2.1 Slag

Another pozzolanic material commonly used to synthesize geopolymer is ground granulated blast furnace slag (GGBFS) resulting from rapid water-cooling of molten steel. It has been used extensively in the concrete industry as a cementitious material since it is relatively inexpensive to obtain, highly resistant to chemical attack, and maintains excellent thermal properties (Dan and Janotka 2003). Major components of the slag product include SiO_2, CaO, MgO, and Al_2O_3. Alkali activation yields a highly amorphous calcium silicate hydrate (C-S-H) gel product with

high aluminum content (Pacheco-Torgal et al. 2007). This product is referred to as alkali-activated slag (AAS). While shrinkage in AAS pastes is more common than in PC, it maintains a much higher ultimate strength by comparison.

2.3 Commonly Used Alkaline Activators

Geopolymer can be synthesized using a wet or dry mixing method. The wet mixing method is the most commonly used method, where the alkali activator is in a liquid solution form. The most commonly used alkaline solution is made by dissolving solid NaOH (sodium hydroxide) into liquid Na_2SiO_3 (sodium silicate or water glass) according to a given molar concentration.

NaOH is a commonly employed to provide OH^-. Its concentration in an activator solution determines the geopolymer paste properties. While high NaOH concentrations accelerate chemical dissolution, its presence depresses ettringite and CH formation during binder formation (Khale et al. 2007). A higher concentration of NaOH promotes higher strength at early stages of the reaction, but the strength of activated geopolymer can be compromised due to excessive OH^- in solution causing non-uniform morphology of the final products (Khale et al. 2007). Researchers have found that geopolymer activated with NaOH developed greater crystallinity, thus improving stability in aggressive environments of sulfates and acids (Criado et al. 2007). There is a linear relationship between NaOH concentration and heat generation (Chareerat et al. 2006).

Sodium silicate is manufactured by fusing silica sand (SiO_2) with sodium carbonate (Na_2CO_3) at temperatures in excess of 1,100°C and dissolving the product with high-pressure steam into a semi-viscous liquid referred to as "water glass" (Fernández-Jiménez and Palomo. 2005). Water glass is rarely used as an independent activating unit because by itself it does not possess enough OH^- for activation potential to initiate pozzolanic reaction. Rather, it is commonly mixed with NaOH as a fortifying agent to enhance alkalinity and increase overall strength. The most utilized alkaline activator in geopolymerization is a combination of sodium hydroxide and sodium silicate (Kong et al. 2003).

2.4 Geopolymer Formulation

Geopolymer proportioning is very complex due to various parameters need to be considered.

2.4.1 Activator Concentration (Concentration)

The alkaline activator concentration (i.e., solute mass concentration) is the most critical factor for successful geopolymer formation and the evolution of high compressive strength. An increase in concentration increases the reaction rate and degree leading to a less porous and stronger geopolymer for the fly ash-based systems (Chareerat et al. 2006). Consequently, a higher alkaline concentration increases setting time and delays polymer formations since excessive ion presence limits polymer mobility and potential to interact with available reactive species. Furthermore, the increase in alkaline concentration in the paste mix increases the degree of

hydration reactions (Pacheco-Torgal et al. 2007) and reduces pore volumes, thus improving the microstructural properties of the C-S-H product. The concentration must be addressed carefully in a geopolymer mix design.

2.4.2 SiO_2 / Na_2O Mole Ratio (Module)

The Module (mole ratio) is a highly significant parameter in geopolymer design. It is well known that variations in Module significantly modify the degree of polymerization of the dissolved species in the reacting solution, thus determining the mechanics and overall properties of the synthesized gel product (Rangan 2008). Higher percentages of soluble silica in geopolymer systems retard dissolution of fly ash due to increased saturation of the ionic silica species and promote the precipitation of larger molecular species, resulting in a stronger gel with an enhanced density (Zuda et al. 2006). The presence of soluble silica directly influences the reaction kinetics and the rate of crystallization as well as promoting gel formation, which is beneficial for strength development. A module range of 1.0 to 2.0 was recommended by Fernández-Jiménez and Palomo (2005). Drying shrinkage is a direct result of hydration heat and it increases with higher module and dosage of water-glass activators (Fernández-Jiménez et al. 2007).

2.4.3 Activator-to-Fly Ash Ratio (L/F)

The ratio of a selected activator-to-aluminosilicate material appeared to be the most critical parameter regarding general strength and fire resistance of the geopolymer paste (Fernández-Jiménez and Palomo, 2005). The liquid activator (L)-to-fly ash (F) ratio, or L/F, is recommended to be maintained in the range of 0.30 to 0.45 (Skvara et al. 2006). High compressive strengths up to 70 MPa were obtained when L/F was lower than 0.43 (Krizan and Zivanovic 2002).

2.5 Curing of Geopolymer

Similar to traditional PC, a geopolymer responds better to elevated temperature curing methods. Previous work has demonstrated that curing time and temperature greatly affect the mechanical development of geopolymer binders. However, a temperature threshold exists beyond which the strength gain rate is extremely slow (Rangan 2008). Temperatures in the range of 50–80°C are widely accepted values used for successful geopolymer hydration. Both curing temperature and curing time directly influence final compressive strength values of geopolymer specimens. Elevated temperature curing methodologies were evaluated on the use of steam- or dry-heat, and the test data show that dry-curing yields a compressive strength increase of 15% over the steam-curing methods (Skvara et al. 2006). Geopolymer sets rapidly and attains a significant percentage of its total compressive strength within the first few hours of reaction (Khale et al. 2007). However, the strength increase for specimens cured beyond 48 hours was not significant. Testing has shown that compressive strength values of 60 MPa can be achieved after only five hours at 85°C (Khale et al. 2007). Longer curing times will increase the geopolymer strength, but the strength develops at a much slower rate as time progresses due to alkaline saturation and product densification (Skvara et al. 2006).

2.6 Mechanical Properties of Geopolymer

As a novel cementitious material, the mechanical properties of geopolymer, including compressive strength, tensile strength, flexural strength, and bond strength, are very important to apply in concrete. Geopolymers exhibit better mechanical properties than PC, which has been perceived as advantageous in previous studies (Palacios et al. 2008, Chindaprasirt et al. 2007). It has been shown that compressive, flexural, and tensile strengths of geopolymers increase as NaOH solution concentration increases (Zivica et al. 2014).

The compressive strength of geopolymer paste has been investigated by researchers who followed ASTM C109 (Hardjito et al. 2008, Karakoca et al. 2014). A tensile strength test is commonly used to determine the strain-hardening behavior of fiber reinforced engineered geopolymer composite (EGC) (Nematollahi et al. 2015). A flexural bending test was carried out to evaluate mechanical properties for fabric-reinforced geopolymer composite (Alomayri et al. 2014). The bond strength between geopolymer and embedded steel, which was essential for geopolymer as a binder in concrete, was measured using a pullout test (Sarker 2011).

Research has suggested that the bond strength of geopolymer concrete is higher than that of PC concrete (Sarker 2011). Recent studies (e.g., Fernández-Jiménez et al. 2006b, Sofi et al. 2007) have reported on similar mechanical properties of geopolymer concrete that are favorable for its use as a construction material. The bonding behavior between the concrete and the reinforcing steel is an important mechanism for the performance of reinforced concrete as a composite material. It is critical to understand the bonding behavior of geopolymer composite in order to use it as an alternative to Portland cement concrete in reinforced concrete structures. Limited research (i.e., pullout tests) has been conducted to assess the bonding strength of fly ash geopolymer mixes (Fernández-Jiménez et al. 2006b, Sofi et al. 2007). Comparable results were derived for both fly ash geopolymer and PC mixes.

2.7 Geopolymer Application

2.7.1 General Applications

One motivator for adopting geopolymer binder is its ability to resist sulfate and other chemical intrusions and maintain excellent thermal loading capacities. The tests reported by Sumajouw et al. (2004) revealed that geopolymer concretes possessed high compressive strength, undergo very little drying shrinkage, and exhibited moderately low creep. Their data also indicated that geopolymer concretes possess excellent resistance to sulfate attack, making them a promising construction option for some harsh environments (Sumajouw et al. 2004).

2.7.2 Engineered Geopolymer Composite (EGC)

Fibers are widely used to modify the brittle behavior of plain cementitious materials (Li and Wu 1992). Engineered cementitious composites (ECC) are a special class of high performance, fiber-

reinforced cementitious composites that utilize a small amount of fibers (typically 2% by volume) and exhibit very high tensile strain capacity of up to 6% (Li and Kanda 1998).

Recent feasibility studies have developed geopolymer-based ECCs that replaced the PC binder with fly-ash-based geopolymer binders. These engineered geopolymer composites (EGCs) demonstrated strain-hardening behavior in tension (Lee et al. 2012). The developed fly-ash-based EGC exhibited very high tensile strain capacity (up to 4.3% on average), but low to moderate compressive and tensile strengths (17.4–27.6 MPa and 2.9–3.4 MPa, respectively). That may limit its widespread application in the construction industry due to its limited ability to withstand load without failure or plastic deformation (Ohno and Li 2014).

Recently, a feasibility study was conducted to develop a geopolymer-based ECC, known as engineered geopolymer composite (EGC), where a fly-ash-based geopolymer binder completely replaced the PC binder. Mechanical test results indicated that the EGC exhibited strain hardening and deflection hardening behaviors (in uniaxial tension and bending, respectively) that were accompanied by multiple cracking behaviors (Ohno and Li 2014). However, their proposed fly-ash-based EGC mixes possessed low compressive and uniaxial tensile strengths, ranging from 17.4 to 27.6 MPa and 2.9 to 3.4 MPa, respectively, compared with typical ECC (50–60 MPa in compressive strength and 4–5 MPa in tensile strength). These low strengths may limit widespread application of these composites in the construction industry. Another study added slag to fly ash-based geopolymer mixes, yielding significantly improved strength (Li and Liu 2007). The study described here aimed to develop EGC mixes called UHPG that showed ultra-high strength and ductility.

2.7.3 Ultra High Performance Geopolymer (UHPG)

Conventional ultra-high-performance concrete (UHPC) is a class of concrete, such as K-UHPC and Ductal UHPC mentioned earlier, that possesses exceptionally high strength (compressive strength of 150–200 MPa and tensile strength of 15 MPa) and durability (extremely permeability and high corrosion resistance). UHPCs often contain significant amounts of Portland cement (800-1000 kg/m^3), highly reactive powders (e.g., silica fume), and high performance fibers, and they are characterized by an extremely dense structure free of capillary pores. Using a similar mix design concept, Ambily et al. (2014) developed an ultra-high-performance geopolymer (UHPG) by eliminating all Portland cement in UHPCs and activating aluminosilicate industrial by-products such as GGBFS and silica fume. They obtained a UHPG with compressive strengths of 175 MPa with steel fibers (1% 6 mm and 2% 13 mm) and 124 MPa without fiber. However, there has been little research reported on fly ash-based UHPG or UHPG. In this study, fly ash was selected as a major aluminosilicate material for UHPG synthetization due to the environmental and economic considerations.

3. EXPERIMENTAL WORK

In this project, laboratory experiments were performed to characterize mechanical properties (compressive and tensile strength, flexural bending, and pullout bond strength) of geopolymer samples prepared in China and at ISU. In addition to mix formulation and mechanical testing, the effect of the curing method on UHPG was also evaluated. The materials, test procedures, and results of the experiments conducted are described below.

(Note: as mentioned previously, a UHPG sample manufactured in China was tested at ISU. The materials and mix proportion of this sample were unknown. The materials and test methods described in the sections below were those used for samples prepared at ISU.)

3.1 Materials

The materials used in laboratory experiments to synthesize UHPG include fly ash (FA), slag, alkali activator, and PVA fibers.

The fly ash (FA) used was low-calcium (Class F) with a specific gravity of 2.61 g/cm3 based on ASTM C618. A ground granulated blast furnace slag with a specific gravity of 2.50 g/cm3 was also employed in this study. The major chemical components of fly ash and slag are shown in Table 3.1, as determined by x-ray fluorescence (XRF). The activator was a combination of NaOH and Na_2SiO_3 (water glass). Their product specifications are listed in Table 3.2. The PVA fibers used in this research were supplied by Kuraray of Japan. The characteristics of the PVA fiber used for the project are presented in Table 3.3.

Table 3.1. Chemical composition of fly ash and slag

	SiO_2	Al_2O_3	Fe_2O_3	SO_3	CaO	MgO	Na_2O	K_2O	Others	LOI
Fly ash	57.06	18.82	5.43	0.45	11.8	2.89	0.64	1.12	1.74	0.03
Slag	36.5	8.54	0.83	0.6	41.1	9.63	0.29	0.44	2.07	2.46

Note: All values in mass %, expressed on an oven-dry basis; LOI: loss on ignition at 1,000°C

Table 3.2. Specification of sodium silicate solution and sodium hydroxide

Product	Sodium silicate solution (Na_2SiO_3)	Sodium hydroxide (NaOH)
Company	Sigma-Aldrich	Fisher Scientific
Grade	Reagent	Certified ACS
Composition	Na_2O: 10.6%, SiO_2: 26.5%	NaOH Solid (≥97%)
Density	1.39 g/ml	2.13g/ml
Formula	$(NaOH)_x(Na_2SiO_3)_yzH_2O$	NaOH

Table 3.3. Properties of PVA fiber

Parameter	Value
Fiber label	RECS 15
Diameter (μm)	40
Length (mm)	12
Young's modulus (GPa)	41
Elongation (%)	6.7
Density (g/cm3)	1.3
Tensile strength (MPa)	1,586

3.2 Mix Proportions

The activator used in this study at ISU was made of solid NaOH, Na_2SiO_3 solution, and tap water at a SiO_2/Na_2O mole ratio (Module) of 1.0 and solute (NaOH and Na_2SiO_3) concentration (Concentration) of 30% (by mass). Four fly ash-based UHPG mixes were prepared with 0%, 10%, 20%, and 30% (by weight) slag replacement for fly ash, and they are denoted as (1) FA-0%S, (2) FA-10%S, (3) FA-20%S, and (4) FA-30%S, respectively. The activator-to-binder (FA and slag) ratio of 0.27 was selected. Two % PVA fibers (by volume) were used to reinforce the UHPG matrix. Table 3.4 presents the mix proportions of fly ash-based UHPG mixes studied.

Table 3.4. Mix proportions of UHPGs

Mix designation	Fly ash	Slag	Activator	PVA fiber
FA-0%S	1.0	-	0.27	0.02
FA-10%S	0.9	0.1	0.27	0.02
FA-20%S	0.8	0.2	0.27	0.02
FA-30%S	0.7	0.3	0.27	0.02

Note: All numbers are mass ratios of fly ash weight except fiber content (volume fraction).

3.3 Mixing Procedure

The mixing procedure began by combining and mixing the binder (i.e., FA and slag) for 2 min in a laboratory Hobart mixer. The alkaline activator solution was prepared 24 hr prior to incorporation into the dry mix. This allowed for dissipation of heat attributed to the exothermic chemical reaction of Na_2SiO_3 and NaOH. The solution was then added gradually to the mixer and mixed for another 3 min to ensure a homogeneous and uniform mixture. In each batch, once a consistent matrix was reached, PVA fibers were gradually added, taking care to ensure uniform fiber dispersion. The whole mixing procedure for each composite generally took 8–10 min.

3.4 Compressive Strength Test

As per ASTM C109, the fresh UHPG was placed and tamped in two layers in 50.8 mm cubic molds. Cast specimens were compacted for 10 s (seconds) on a vibrating table. All UHPG

specimens were subjected to heat curing by having all molds sealed to minimize moisture loss and placed in an oven at 50°C for 24 hr. At the end of the heat curing period, the specimens were removed from the molds and cured in the oven at 50°C until the day of testing. All UHPG specimens were tested at 3 days, 7 days, and 28 days after casting. For each testing, three replicates were tested in order to check the variability of performance under compression.

3.5 Tensile Strength Test

Uniaxial tension tests were conducted to evaluate the tensile behavior of the developed fly ash-based UHPGs as shown in Figure 3.1(a). For each mix, two composite panels in the shape of dog bones were cast and cured for 28 days in the same environmental conditions as specimens prepared for compressive strength. The schematic of the test specimen and apparatus is illustrated in Figure 3.1(b).

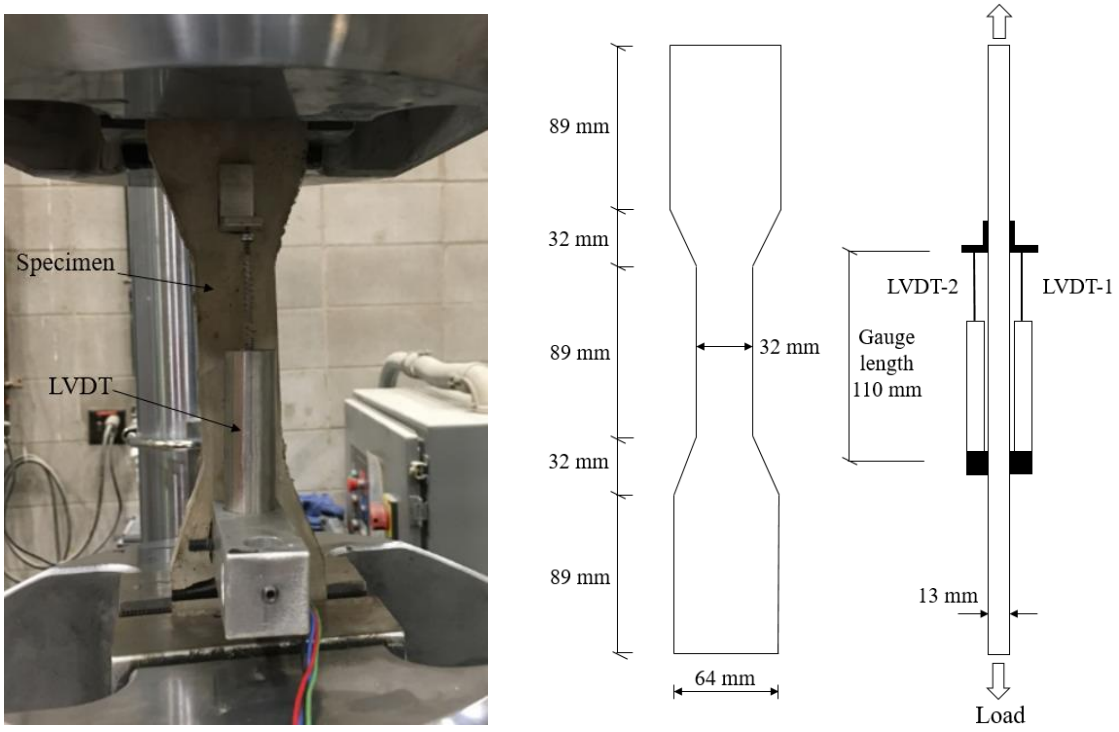

(a) UHPG specimen under tensile test (b) Schematic of tensile test

Figure 3.1. Uniaxial tension test setup

All specimens were tested in uniaxial tension under displacement control using a mechanical testing system (MTS) testing machine with hydraulic wedge grips. In accordance with the Japan Society of Civil Engineers (JSCE 2008) recommendations, the displacement rate was 0.5 mm/min. Panel specimens were polished on the two ends to facilitate gripping. Specimens were in proper alignment with the machine hydraulic grips. The MTS machine had a fully digital control panel and software to automatically run the tests and collect the load. In addition, two linear variable differential transformers (LVDTs) were employed to measure displacements between two points on the specimen with a gauge length of 110 mm, as shown in Figure 3.1(b).

Resulting load versus displacement data were recorded, and tensile stress versus strain curves were plotted.

According to previous studies on micromechanical design of conventional ECCs (Kanda and Li 1999), criteria (i.e., stress-based condition) must be satisfied in order to achieve pseudo-strain hardening (PSH) behavior accompanied by multiple fine cracks. The stress-based condition can be expressed as:

$$\sigma_{fc} \leqslant \sigma_0 \quad (1)$$

where σ_0 = maximum fiber bridging stress (i.e., ultimate tensile strength of the composite) and σ_{fc} = tensile first-crack strength of the composite. Figure 3.2 illustrates the typical stress (σ) versus strain (ε) curves for strain hardening behavior. According to the stress-based condition, if σ_0 exceeds σ_{fc}, multiple cracking occurs with increasing load. Otherwise, the composite immediately fails after the initiation of first crack from a defect site.

In accordance with the stress condition for PSH behavior, Kanda and Li proposed a performance index σ_0/σ_{fc} (Kanda and Li 2006). Theoretically, this index must exceed unity to achieve PSH behavior in a fiber-reinforced composite. The higher the performance index value, the greater the possibility of saturated multiple cracking or saturated PSH behavior, resulting in a higher tensile strain capacity of the composite. The area under the stress-strain curve up to failure can be derived as the tensile toughness of the UHPG, which is an indication of the total energy absorption capacity of the material. The tensile toughness and the tensile elasticity (the slope of the elastic portion, i.e., $\sigma_{fc}/\varepsilon_{fc}$) of UHPG were derived from the stress-strain curve as shown in Figure 3.2.

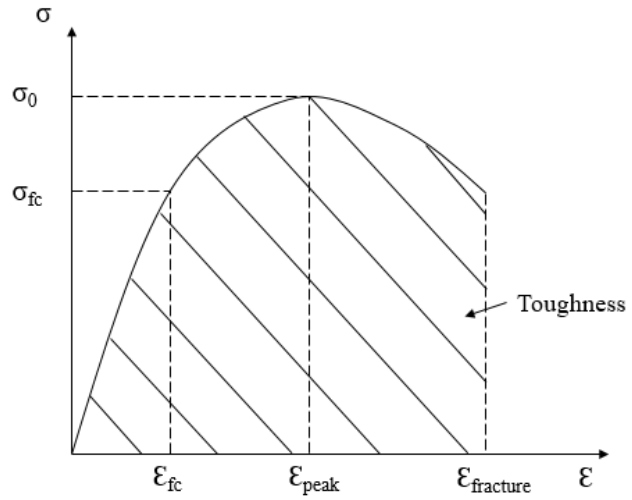

Figure 3.2. Typical stress/strain curve of strain hardening composites

3.6 Flexural Bending Test

A four-point flexural bending test was carried out on the UHPG overlay slab to evaluate flexural bending behavior of UHPG mixtures as illustrated in Figure 3.3(a).

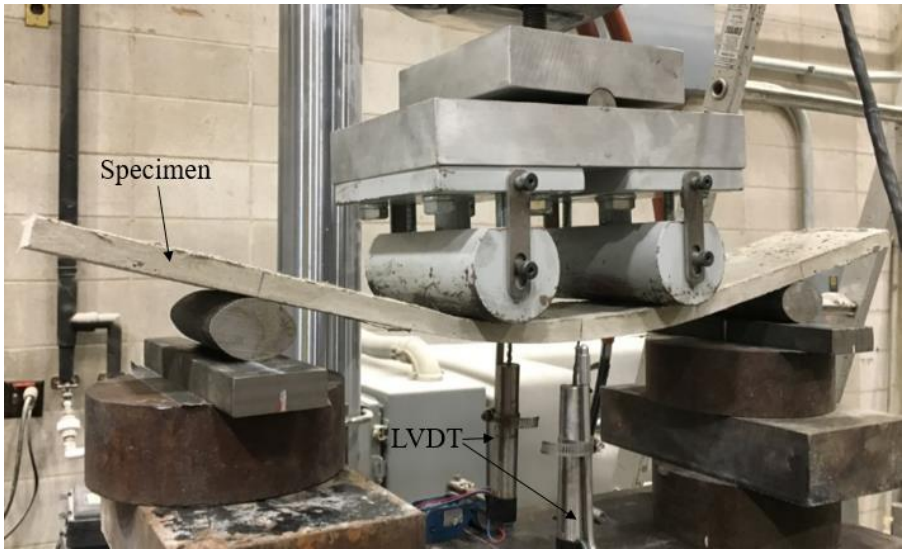

(a) UHPG specimen under bending test

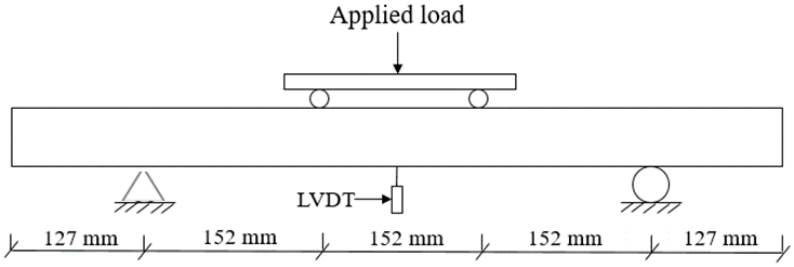

(b) Schematic illustration of bending test

Figure 3.3 Four-point flexural bending test setup

For each mix, two slabs with the dimensions of 711 × 108 × 13 mm were cast and cured similarly to the cube specimens for 28 days before testing. Each slab was loaded under four-point bending with a span of 457 mm between supports and loading was applied symmetrically at 152 mm from the supports using an MTS testing machine. The loading configuration is shown in Figure 3.3(b). Two LVDTs were employed to monitor the midspan deflection of the slab from both sides. In accordance with Martin et al. (2007) and Sarker et al. (2013), the displacement control rate was 0.2 cm/min until its failure.

According to the four-point flexural bend model, when the loading span is one-third of the support span, the flexural stress could be calculated following Equation 2:

$$\sigma = \frac{FL}{bd^2} \quad (2)$$

where σ is flexural stress, F is the load at the fracture point, L is the length of the support span, b is the width of the slab, and d is the thickness of the slab.

3.7 Pullout Bond Strength Test

The direct tension pullout bond test was conducted to investigate the bond strength of the steel bar embedded in UHPGs as shown in Figure 3.4(a). All specimens were tested under a displacement control rate of 0.3 mm/min in accordance with Qian and Li. (2011). A schematic of the pullout test setup is shown in Figure 3.4(b).

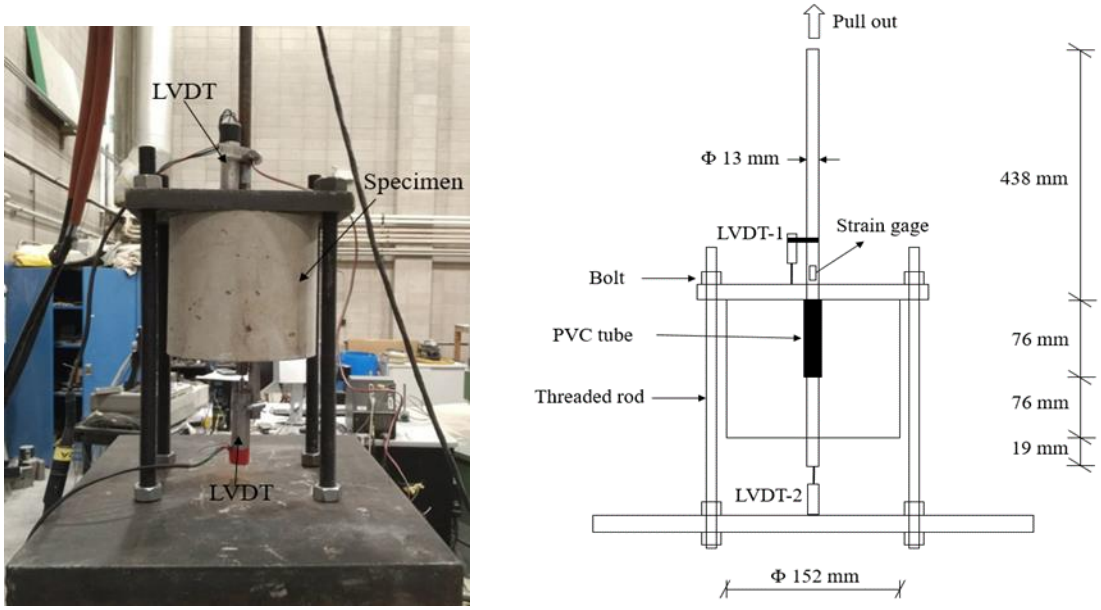

(a) UHPG specimen under pullout test (b) Schematic of pullout test

Figure 3.4. Pullout bond strength test setup

For each mix, two cylinders of Φ152 × 152 mm (Φ=diameter) with a Φ13 × 609 mm smooth steel bar embedded in the center of specimen were cast and cured similar to the cube specimens for 28 days before testing. The properties of the steel bar used are shown in Table 3.5.

Table 3.5. Properties of steel bar used

Diameter (mm)	Length (mm)	Yield strength (MPa)	Ultimate strength (MPa)	Elongation (%)
12.6	609.6	531	680	16

The steel bar was covered by a 76 mm long polyvinyl chloride (PVC) tube along the top half of cylinder (where the steel bar is free to move), and embedded all the way through the cylinder with 19 mm out of specimen bottom as shown in Figure 3.4(b). Therefore, the effective bond length between the UHPG and steel bar is 76 mm. The reason for the use of the PVC tube

covering is to avoid stress concentration on the UHPG during pullout. During the test, the top of the steel bar was gripped by the wedge on the MTS machine. An alloy plate was placed on the top surface of the UHPG cylinder using four bolts tightened on four threaded rods to fix the UHPG cylinder as seen in Figure 3.4(b). The steel bar was subjected to a tensile force that is transferred to the UHPG as tensile stresses throughout the bond stresses between the UHPG and the steel.

An average result of two specimens was derived for each UHPG mix. The bar slip was recorded until failure by the two LVDTs installed on the two sides of cylinder. In order to compensate for the displacement on the steel bar itself caused by tension, a micro-strain gauge was pre-installed on the steel bar surface. The strain of the steel during the pullout test was recorded by a data logger until failure occurred. The bond stress was computed using Equation 3:

$$\tau = P/(\pi L_e d_b) \quad (3)$$

where τ is the bond stress, P is the load, L_e is the contacted length of the bar in UHPG, and d_b is the bar diameter. The slip of bar(s) was calculated according to Equation 4:

$$s = d_L - \varepsilon \times L_e \quad (4)$$

where d_L is the displacement of bar measured by LVDT, and ε is the microstrain of bar obtained from the strain gauge.

3.8 Curing Methods

The curing method significantly influences the UHPG performance. To obtain high strength in fly ash geopolymer, a curing temperature of 40–75°C is normally required (Kovalchuk et al. 2007). This high temperature can be used to make the building block; however, it is difficult to construct at these temperatures in field construction practices. A number of researchers, therefore, have tried to study the strength development of fly ash geopolymer under the ambient temperature (Temuujin et al. 2010, Guo et al. 2010).

In this study, four different curing methods were employed on FA-20% cylindrical specimens sized at Φ3×L6 in. as described below:

1. 1 day in cast mold at 23°C, and 7 days in steam curing tank at 50°C (1 day in mold)

2. 2 days in cast mold at 23°C, and 7 days in steam curing tank at 50°C (2 days in mold)

3. 3 days in cast mold at 23°C, and 7 days in steam curing tank at 50°C (3 days in mold)

4. 7 days in steam curing tank at 50°C (mold in steam)

After curing, two specimens for each curing method were tested on compressive strength at a loading rate of 35 psi/sec according to ASTM C39 (the standard test method for compressive strength of cylindrical concrete specimens) as presented in Figure 3.5.

Figure 3.5. Compressive strength test setup

The strain was obtained from the test using 2 horizontal and 2 vertical micro-strain gauges as shown in Figure 3.6.

Figure 3.6. Strain gauges on specimen

The results were expressed with the average value obtained from each set of the two strain gauges.

4. RESULTS AND DISCUSSION

Only one Φ100 mm × 200 mm (4 × 8 in.) cylinder sample was received from China. It was used for the compressive strength test. Other test results presented in the sections that follow are from samples designed, prepared, and tested at ISU.

4.1 Compressive Strength

4.1.1 Sample Made in China

Figure 4.1 presents the compressive strength test result of the UHPG sample made in China.

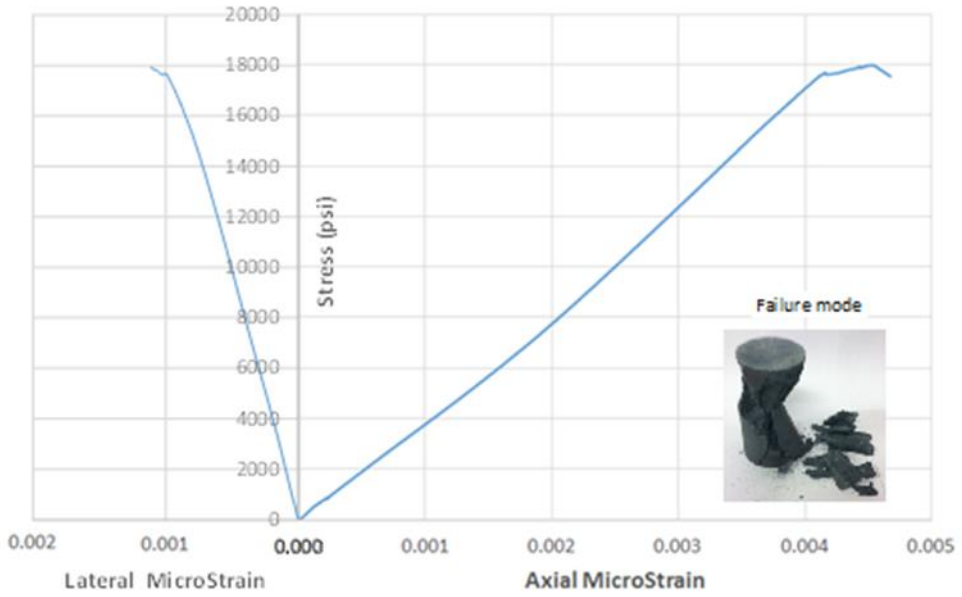

Figure 4.1. Strain-stress behavior of UHPG sample made in China under compression

The figure shows that the sample displayed linear strain-stress behavior with a little post-crack strain hardening behavior. The sample had ultimate stress, compressive strength, of 123 MPa (17,868 psi), and maximum compressive strain of 0.0047 microstrains.

4.1.2 Samples Made at ISU

The compressive strength of UHPGs made at ISU was tested on cubic samples, and the results are presented in Figure 4.2.

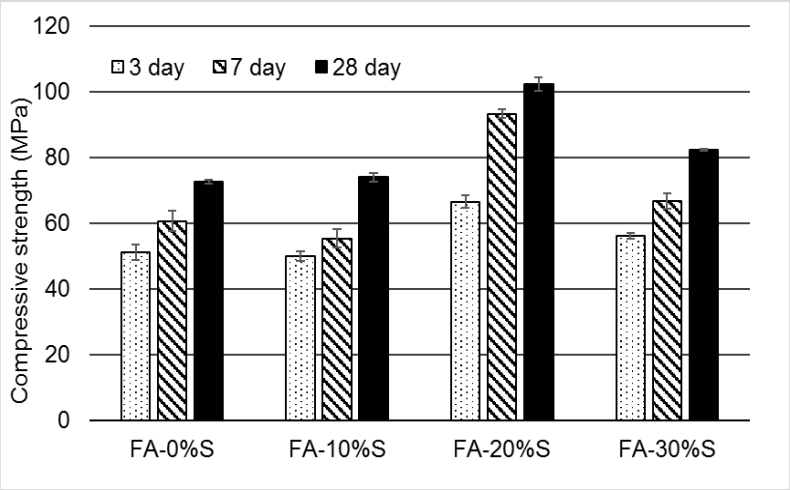

Figure 4.2. Compressive strength of UHPGs made at ISU

The 20% slag UHPG mix exhibited the highest compressive strength at all testing ages, which is likely due to the production of aluminosilicate hydrate and calcium silicate hydrate gels (Palomo 1999, Chi 2012). However, further replacement of slag to a level of 30% led to decreased compressive strength. This is consistent with a previous report that attributed the decreased strength to the presence of excessive Ca as the slag undergoes a hydration reaction forming $Ca(OH)_2$ which might lead to expansion (Wardhono et al. 2017). The compressive strength of 10% slag replacement UHPG mix only slightly increased at 28 days compared to 0% slag cement replacement mix. The same trend on compressive strength with different percentages of slag replacement has been reported previously (El-Hassan and Ismail 2018).

4.2 Tensile Strength

Tensile stress-strain behaviors of the UHPG mixes are presented in Figure 4.3.

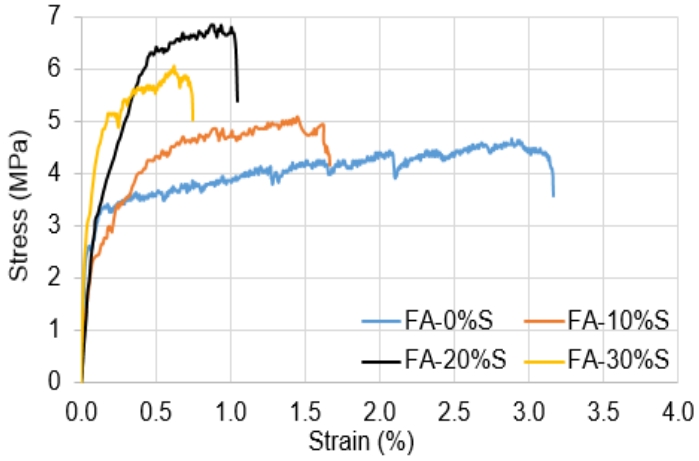

(a) Full stress-strain curve

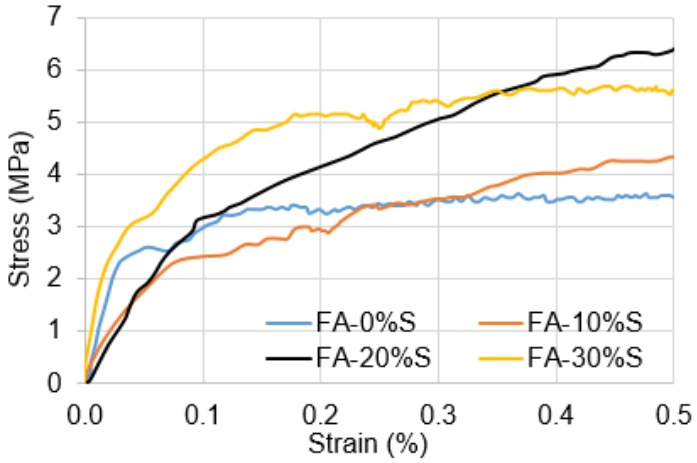

(b) Initial stress-strain curve (strain = 0~0.5% in (a))

Figure 4.3. Tensile stress-strain responses of UHPGs

All UHPGs exhibited strain-hardening behavior accompanied by multiple cracking because of the bridging mechanism of the PVA fibers. The uniaxial tensile strength of the UHPG mixes with slag additions developed in this study are higher than those of the slag-based UHPGs developed by Lee et al. (2012) and the fly ash-based UHPGs developed by Ohno and Li (2014).

The first-crack strength (σ_{fc}), tensile elasticity, ultimate tensile strength (σ_0), tensile strain capacity, toughness, and stress index (σ_0/σ_{fc}) of each mix are listed in Table 4.1.

Table 4.1. Tensile strength test results

Mix	σ_{fc} (MPa)	Tensile elasticity (GPa)	σ_0 (MPa)	Tensile strain capacity (%)	Toughness (J/cm^3)	Stress index (σ_0/σ_{fc})
FA-0%S	3.4	1.18	4.7	3.14	12.6	1.38
FA-10%S	4.2	1.41	5.1	1.62	6.9	1.21
FA-20%S	5.7	1.58	6.8	1.04	5.5	1.19
FA-30%S	5.2	2.98	6.1	0.74	3.7	1.17

The ultimate tensile strengths of all the UHPG mixes were significantly higher than the first crack strength. FA-20%S exhibited the highest first-crack strength which corresponds to its highest ultimate tensile strength. The first-crack strength of FA-30%S, FA-10%S, and FA-0%S were 16.1, 32.3, and 45.2% lower, respectively. The ultimate tensile strengths of FA-30%S, FA-10%S, and FA-0%S were 10.3, 25.0, and 30.9% lower, respectively, than that of FA-20%S. The decrease in the ultimate tensile strength could be due to the interfacial properties. In other words, the chemical bonding energy and the frictional bond strength of FA-20%S increased more than the cracking strength compared to the other UHPG composites, resulting in higher fiber-bridging strength (Lee et al. 2012). However, the tensile elasticity increased with the increments of slag addition up to 2.98 GPa for FA-30%S which is attributed to C-A-S-H gel formed through the activation of slag leading to reduce porosity (Criado et al. 2016). Among all UHPGs, FA-0%S exhibited the highest tensile strain capacity.

With slag content increasing, the tensile strain capacity decreased. One of the reasons for this considerable reduction in tensile strain capacities with slag additions lies in their different stress indices. The stress index of FA-0%S was the highest among the UHPGs. In addition, the stress indices of FA-10%S, FA-20%S, and FA-30%S were 12.3%, 13.8%, and 15.2% lower, respectively, than that of FA-0%S. As mentioned previously, the higher the stress index value, the greater the possibility of saturated PSH behavior, which results in a higher tensile strain capacity of the composite. Therefore, the stress-based condition for PSH behavior (i.e., Equation [1]) is satisfied. The toughness results also revealed that with slag increased from 0% to 30%, toughness decreased from 12.6 to 3.7 $J/cm^{3,}$ which means that the energy absorption of the UHPG decreased as slag content increased. This trend corresponds to tensile strain capacity. Generally, the incorporation of slag implied that the UHPGs exhibited a low ductility and toughness but showed a high ultimate tensile strength.

The multiple cracking patterns of each mix are presented in Figure 4.4.

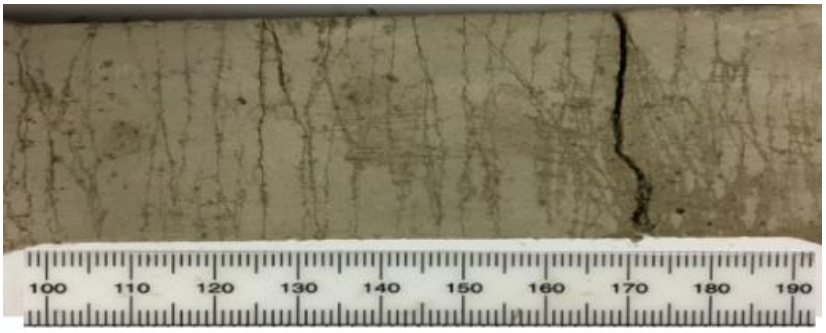

FA-0%S

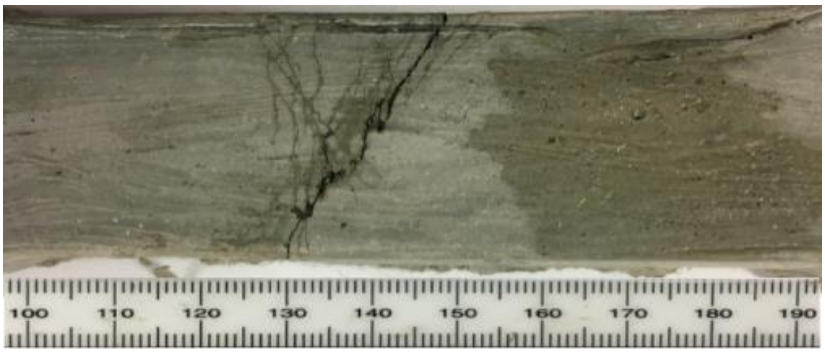

FA-20%S

Figure 4.4. Cracking behavior of UHPG with and without slag under tension

After unloading, a clear trace of all visible cracks was obtained by water spray. The FA-0%S mix without a slag cement addition exhibited uniform and enormous micro-cracks distribution with a tightly controlled crack width (i.e., saturated cracking behavior), which corresponded to its significantly higher tensile strain capacity. However, with the increased addition of slag (from 10% to 30%), the crack spacing was bigger, and the crack distribution was not uniform (i.e., unsaturated cracking behavior). As slag content increased, the UHPG tended to be more brittle.

4.3 Flexural Bending Strength

The stress-deflection curves of the flexural bending test are shown in Figure 4.5.

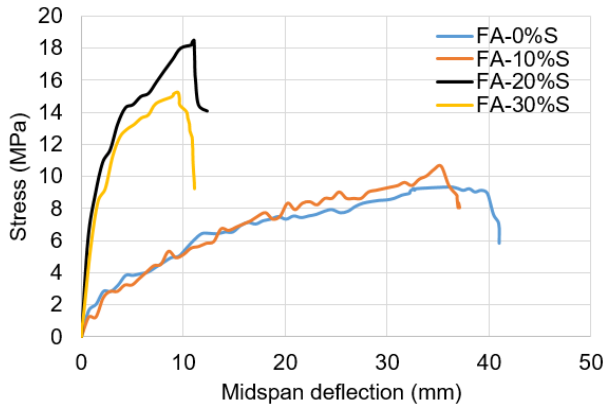

Figure 4.5. Flexural stress-deflection responses of UHPGs

The stress deflection of all UHPGs was reinforced with PVA. It was found that for the 20% and 30% slag additions to the UHPG, the material demonstrated relatively brittle behavior, and the stress decreased rapidly at around 10 mm midspan deflection. However, for the FA-0%S and FA-10%S, the curves were flatter, and the midspan deflection increased up to 39.81 and 35.32 mm respectively. Moreover, the pseudo-hardening responses that appeared generally were much more dependent on the slag addition.

In the four-point bending test, the ductility index can be obtained as the ratio of mid-span deflection at failure to that at the first crack (Jaejer et al. 1997). A greater ductility index indicates better ductility. A summary of modulus of rupture (MOR), deflection at first crack (D_{fc}), deflection at failure (D_{fl}), and ductility index (D_{fl}/D_{fc}) is reported in Table 4.2.

Table 4.2. Flexural strength test results

Mix	MOR (MPa)	D_{fc}, (mm)	D_{fl}, (mm)	Ductility index
FA-0%S	9.3	1.26	39.81	31.6
FA-10%S	10.4	1.41	35.32	25.0
FA-20%S	18.5	2.07	11.03	5.3
FA-30%S	15.3	1.60	9.46	5.9

Slag replacement increased MOR. Among the 3% of added slag, the mix with 20% slag had the highest MOR, while the mix with 0% slag showed the lowest MOR. This finding corresponded to compressive strength results. The mid-span deflection at first crack increased as the MOR rose. The maximum mid-span deflection at failure reached 39.81 mm without slag and it declined as the slag addition increased. A 68.8% reduction in mid-span deflection at failure was observed, especially following the 10% to 20% slag addition. The data showed that ductility decreased with an increment of slag content. FA-0%S produced the highest ductility index value.

However, the ductility characteristics were dramatically reduced from a 10% to 20% slag addition. It should be noted that FA-20%S generated the lowest flexural ductility.

In order to show multiple cracks clearly, water was used to dampen the surface of failure specimens. Multiple cracks were uniformly distributed along the bending moment for all UHPGs (Figure 4.6).

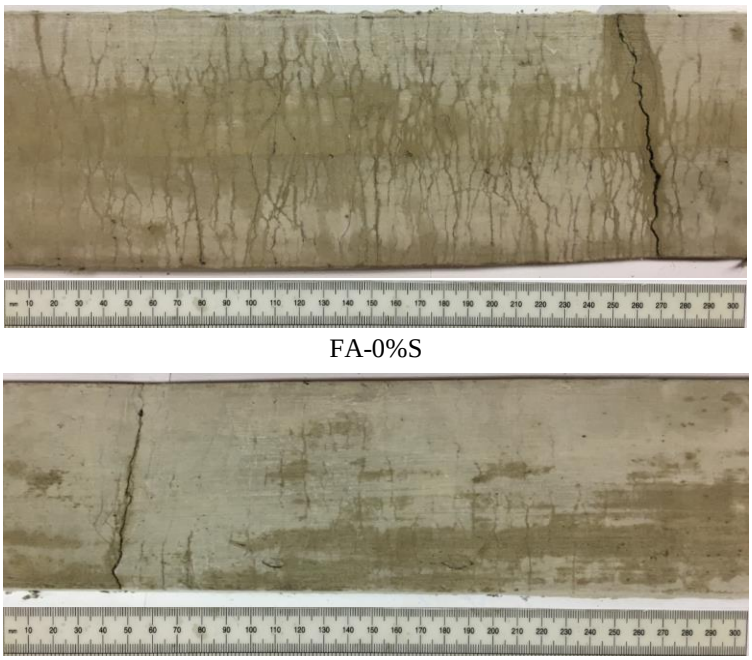

FA-0%S

FA-20%

Figure 4.6. Cracking pattern of UHPGs with and without slag under flexural loading

The number of cracks declined and their spacing increased as slag content increased. The cracking pattern also indicated that the UHPGs had very good deflection hardening properties.

4.4 Pullout Bond Strength

Figure 4.7 shows the bond stress-slip relationship for UHPG specimens.

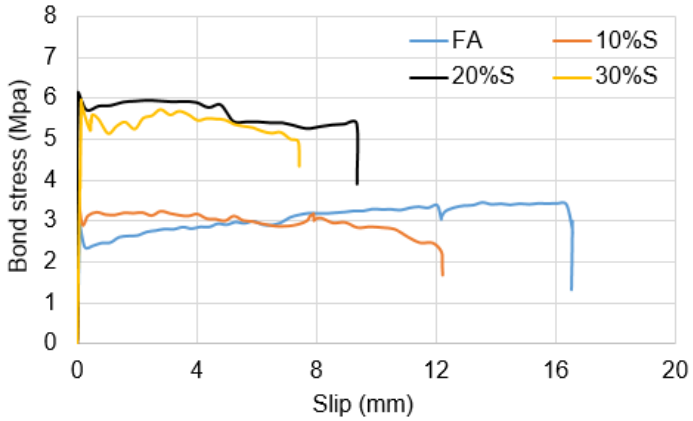

Figure 4.7. Bond stress-slip relationships for UHPGs

All UHPG mixes exhibited a pullout mode of failure with post-peak slip development. After the peak load, the pullout load dropped a little quicker, however, it still maintained constant bond stress until complete failure. These mixes showed low bond stress reduction with slip as evidenced by a high ductility measurement after peak load. This behavior indicated certain improvements in bond strength with some enhanced post-peak behavior (more ductility) due to high fiber confinement. The ultimate bond strength (τ_u), ultimate slip (s_u), and compressive strength (f_{cu}) of the UHPGs are listed in Table 4.3.

Table 4.3. Pullout bond strength test results

Mix	τ_u, (MPa)	s_u, (mm)	f_{cu}, (MPa)
FA-0%S	3.5	16.3	72.6
FA-10%S	3.7	11.9	73.9
FA-20%S	6.2	9.4	102.3
FA-30%S	5.9	7.4	82.3

It is obvious that the bond strength of FA-20%S is the highest, and FA-0%S is the lowest, consistent with compressive strength levels. This is associated with the decreased porosity in the interfacial zone, which can lead to an increase of the fiber-matrix contact surface, resulting in a higher frictional bond (Kim et al. 2007). Moreover, the ultimate slip was reduced significantly as the slag content increased. This also revealed that the slag addition could decrease ductility of the UHPG.

4.5 Effect of Curing on Compressive Strength

The effect of curing condition on the compressive strength of UHPG FA-20%S is illustrated in Figure 4.8, where each curve represents the average results of two strain gauges of the tested sample.

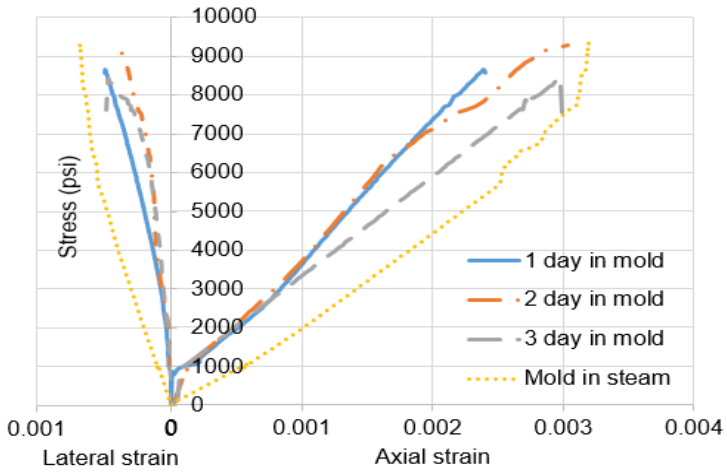

Figure 4.8. Stress and strain curve of UHPG FA-20%S under different curing conditions

It indicated that the specimen cured in steam at 50°C had the highest strength. Generally, the specimens of these different curing methods exhibited similar strength and compressive behavior. The strain in both lateral and axial directions is also similar. Steam curing at 50°C is the best curing method for UHPG.

5. CONCLUSIONS AND RECOMMENDATIONS

This study developed new types of UHPGs with different slag replacements and fiber additions to improve mechanical properties and ductility, respectively. The effects of slag replacement of up to 30% on mechanical properties of UHPG (i.e., compressive strength, tensile strength, flexural bending strength, and pullout bond strength) were determined. Tensile strain capacity, toughness, and ductility of fly ash/slag blended UHPGs were assessed.

The main conclusions of this study were as follows:

- The UHPG sample made in China and tested at ISU showed a compressive strength of 123 MPa (17,868 psi) and maximum compressive strain of 0.0047 micro-strain.

- The mix design study prepared at ISU revealed that the compressive strength of fly ash based UHPG could be enhanced by replacing fly ash with GGBFS or slag. However, the optimal slag content was 20%. The UHPG samples made with 20% slag replacement for fly ash and a liquid (activator solution)-to-binder (slag and fly ash) of 0.27 had a 28-day compressive strength of 102 MPa (14,800 psi), about 20% lower than that of UHPG sample made in China.

- When reinforced with 2% (by volume) PVA fiber, the UHPG mixes developed at ISU (with 0 to 30% slag replacement for fly ash) exhibited strain and displacement hardening behavior in tension and flexure, indicating significant ductility.

- Replacement of slag for fly ash improved strengths and elastic modulus of UHPG, but noticeably reduced the deflection at failure and ductility of UHPG.

- As slag content increased, the bond strength between the geopolymer and steel rebar improved. The UHPG samples with 20% slag replacement had a 77.1% increase in bond strength when compared with that of pure fly ash UHPG.

- Among the curing methods used, steam curing at 50°C appeared to be the best condition for UHPG strength development.

The following recommendations are proposed based on the project observations and conclusions:

- Due to the short time period for the project, only a limited number of UHPG mixes were studied. Although the ISU UHPG achieved very good strength (102 MPa or 14,800 psi), it was still lower than that of the sample from China. Further studies could show how to increase the density and reduce the porosity of the ISU UHPG.

- The UHPG samples made at ISU were cured at an elevated temperature (50°C). In consideration of field use conditions, ambient temperature curing for the strength development of UHPG should be studied in order to reduce the cost of curing.

- This study focused only on the mechanical properties of UHPG. Although geopolymers were reported to have excellent chemical resistance, the durability properties of UHPG, such as freezing and thawing resistance, should be studied for potential use in Iowa.

REFERENCES

Alomayri, T., L. Vickers, F. U. A. Shaikh, and I. M. Low. 2014. Mechanical Properties of Cotton Fabric Reinforced Geopolymer Composites at 200–1000°C. *Journal of Advanced Ceramics*, Vol. 3, No. 3, pp. 184–193.

ASTM C39/C39M. 2003. *Standard Test Method for Compressive Strength of Cylindrical Concrete Specimens*. ASTM International, West Conshohocken, PA.

ASTM C109/C109M. 2016. *Standard Test Method for Compressive Strength of Hydraulic Cement Mortars (Using 2-in. or [50-mm] Cube Specimens*). ASTM International, West Conshohocken, PA.

ASTM C618. 2012. *Standard Specification for Coal Fly Ash and Raw or Calcined Natural Pozzolan for Use in Concrete*. ASTM International, West Conshohocken, PA.

Chareerat, T., A. Lee-Anansaksiri, and P. Chindaprasirt. 2006. Synthesis of High Fly Ash and Calcined Kaolin Geopolymer Mortar. Paper presented at International Conference on Pozzolan, Concrete and Geopolymer, May 24–25, Khhon Kaen, Thailand.

Chi, M. 2012. Effects of Dosage of Alkali-Activated Solution and Curing Conditions on the Properties and Durability of Alkali-Activated Slag Concrete. *Construction and Building Materials*, Vol. 35, pp. 240–245.

Chindaprasirt, P., T. Chareerat, and V. Sirivivatnanon. 2007. Workability and Strength of Coarse High Calcium Fly Ash Geopolymer. *Cement and Concrete Composites*, Vol. 29, No. 3, pp. 224–229.

Criado, M., W. Aperador, and I. Sobrados. 2016. Microstructural and Mechanical Properties of Alkali Activated Colombian Raw Materials. *Materials*, Vol. 9, No. 3, pp. 158–173.

Criado, M., A. Fernández-Jiménez, A. G. de la Torre, M. A. G. Aranda, and A. Palomo. 2007. An XRD Study of the Effect of the SiO_2/Na_2O Ratio on the Alkali Activation of Fly Ash. *Cement and Concrete Research*, Vol. 37, No. 5, pp. 671–679.

Dan, E. and I. Janotka. 2003. Chemical Resistance of Portland cement, Blast-Furnace Slag Portland cement and Sulphoaluminate-Belite Cement in Acid, Chloride and Sulphate Solution: Some Preliminary Results. *Ceramics-Silikaty*, Vol. 47, No. 4, pp. 141–148.

Davidovits, J. 1994. Properties of geopolymer cements. Proceedings of the First International Conference on Alkaline Cements and Concretes, Scientific Research Institute on Binders and Materials, Kiev State Technical University, Kiev, Ukraine, pp. 131–149.

Duxson, P., A. Fernández-Jiménez, J. L. Provis, G. C. Lukey, A. Palomo, and J. S. J. van Deventer. Geopolymer Technology: The Current State of the Art. J*ournal of Materials Science*, Vol. 42, No. 9, pp. 2917–2933.

El-Hassan, H. and N. Ismail. 2018. Effect of Process Parameters on the Performance of Fly Ash/GGBS Blended Geopolymer Composites. *Journal of Sustainable Cement-Based Materials*, Vol. 7, No. 2, pp. 122–140.

Fernández-Jiménez, A., I. Garcia-Lodeiro, and A. Palomo. 2007. Durability of Alkali-Activated Fly Ash Cementitious Materials. *Journal of Materials Science*, Vol. 42, No. 9, pp. 3055–3065.

Fernández-Jiménez, A. and A. Palomo. 2005. Composition and Microstructure of Alkali Activated Fly Ash Binder: Effect of the Activator. *Cement and Concrete Research*, Vol. 35, No. 10, pp. 1984–1992.

Fernández-Jiménez, A., A. Palomo, and M. Criado. 2005. Microstructure Development of Alkali-Activated Fly Ash Cement: A Descriptive Model. *Cement and Concrete Research*, Vol. 35, No. 6, pp. 1204–1209.

Fernández-Jiménez, A., A. Palomo, I. Sobrados, and J. Sanz. 2006a. The Role Played by the Reactive Alumina Content in the Alkaline Activation of Fly Ashes. *Microporous and Mesoporous Materials*, Vol. 91, No. 1–3, pp. 111–119.

Fernández-Jiménez, A. M., A. Palomo, and C. Lopez-Hombrados. 2006b. Engineering Properties of Alkali-Activated Fly Ash Concrete. *ACI Materials Journal*, Vol. 103, No. 2, pp. 106–112.

Guo, X. L., H. S. Shi, and W. A. Dick. 2010. Compressive Strength and Microstructural Characteristics of Class C Fly Ash Geopolymer. *Cement and Concrete Composites*, Vol. 32, No. 2, pp. 142–147.

Hardjito, D., C. C. Cheak, and C. H. L. Ing. 2008. Strength and Setting Times of Low Calcium Fly Ash-based Geopolymer Mortar. *Modern Applied Science*, Vol. 2, No. 4, pp. 3–11.

Jaejer, L.G., A. A. Mufti, and G. Tadros. 1997. The Concept of the Overall Performance Factor in Rectangular-Section Reinforced Concrete Beams. Proceedings of the 3rd International Symposium on Non-metallic (FRP) Reinforcement for Concrete Structures, October 14–16, Sapporo, Japan, pp. 551–558.

Japan Society of Civil Engineers. 2008. *Recommendations for Design and Construction of High Performance Fiber Reinforced Cement Composites with Multiple Fine Cracks (HPFRCC).* Testing Method 2. JSCE Concrete Engineering Series 82, pp. 6–10. https://www.jsce.or.jp/committee/concrete/e/hpfrcc_JSCE.pdf

Kanda, T. and V. C. Li. 1999. New Micromechanics Design Theory for Pseudo-strain Hardening Cementitious Composite. *Journal of Engineering Mechanics*, Vol. 125, No. 4, pp. 373–381.

Kanda, T. and V. C. Li. 2006. Practical Design Criteria for Saturated Pseudo Strain Hardening Behavior in ECC. *Journal of Advanced Concrete Technology*, Vol. 4, No.1, pp. 59–72.

Karakoca, M.B., I. Turkmen, M. M. Maras, F. Kantarci, R. Demirboga, and M. U. Toprak. 2014. Mechanical Properties and Setting Time of Ferrochrome Slag Based Geopolymer Paste and Mortar. *Construction and Building Materials*, Vol. 72, pp. 283–292.

Khale, D. and R. Chaudhary. 2007. Mechanism of Geopolymerization and Factors Influencing Its Development: A Review. *Journal of Materials Science*, Vol. 42, No. 3, pp.729–746.

Kim, J., J. Kim, G. Ha, and Y. Kim. 2007. Tensile and Fiber Dispersion Performance of ECC (Engineered Cementitious Composites) Produced with Ground Granulated Blast Furnace Slag. *Cement and Concrete Research*, Vol. 37, No. 7, pp. 1096–1105.

Kong, H-J., S. G. Bike, and V. C. Li. 2003. Development of a Self-consolidating Engineered Cementitious Composite Employing Electrosteric Dispersion/Stabilization. *Cement & Concrete Composites*. Vol. 25, No. 3, pp. 301–309.

Kovalchuk, G., A. Fernández-Jiménez, and A. Palomo. 2007. Alkali-activated fly ash: Effect of thermal curing conditions on mechanical and microstructural development—Part II. *Fuel*, Vol. 86, No. 3, pp. 315–322.

Krizan, D. and B. Zivanovic. 2002. Effects of Dosage and Modulus of Water Glass on Early Hydration of Alkali-Slag Cements. *Cement and Concrete Research*, Vol. 32, No. 8, pp. 1181–1188.

Lee, B. Y., C-G. Cho, H-J. Lim, J-K. Song, K-H. Yang, and V. C. Li. 2012. Strain Hardening Fiber Reinforced Alkali-Activated Mortar—A Feasibility Study. *Construction and Building Materials*, Vol. 37, pp.15–20.

Li, V. C. and T. Kanda. 1998. Engineered Cementitious Composites for Structural Applications. *Journal of Materials in Civil Engineering*. Vol. 10, No. 2, pp. 66–69.

Li, V. C. and H-C. Wu. 1992. Conditions for Pseudo Strain-hardening in Fiber Reinforced Brittle Matrix Composites. *Applied Mechanics Reviews*, Vol. 45, No. 8, pp. 390–398.

Li, Z. and S. Liu. 2007. Influence of Slag as Additive on Compressive Strength of Fly-ash-based Geopolymer. *Journal of Materials in Civil Engineering*, Vol. 19, No. 6, pp. 470–474.

Martin, J., J. Stanton, N. Mitra, and L. N. Lowes. 2007. Experimental Testing to Determine Concrete Fracture Energy Using Simple Laboratory Test Setup. *ACI Materials Journal*, Vol. 104, No. 6, pp. 575–584.

McDonald, M. and J. L. Thompson. n.d. *Sodium Silicate: A Binder for the 21st Century*. The PQ Corporation, Industrial Chemicals Division, Valley Forge, PA.

Nematollahi, B., J. Sanjayan, and F. Shaikh. 2015. Tensile Strain Hardening Behavior of PVA Fiber-Reinforced Engineered Geopolymer Composite. *Journal of Materials in Civil Engineering*, Vol. 27, No. 10, pp. 04015001-1–04015001-12.

Ohno, M. and V. C. Li. 2014. A Feasibility Study of Strain Hardening Fiber Reinforced Fly ash-based Geopolymer Composites. *Construction and Building Materials*, Vol. 57, pp. 163–168.

Pacheco-Torgal, F., J. Castro-Gomes, and S. Jalali. 2007. Alkali-Activated Binders: A Review. Part 2. About Materials and Binders Manufacture. *Construction and Building Materials* Vol. 22, No. 7, pp. 1315–1322.

Palacios, M., P. F. G. Banfill, and F. Puertas. 2008. Rheology and Setting of Alkali-Activated Slag Pastes and Mortars: Effect of Organic Admixture. *ACI Materials Journal*, Vol. 105, No. 2, pp. 140–148.

Palomo, A., M. W. Grutzeck, and M. T. Blanco. 1999. Alkali-Activated Fly Ashes: A Cement for the Future. *Cement and Concrete Research*, Vol. 29, No. 8, pp. 1323–1329.

Petermann, J. C., A. Saeed, and M. I. Hammons. 2010. *Alkali-Activated Geopolymers: A Literature Review*. Air Force Research Laboratory, Materials and Manufacturing Directorate, Tyndall Air Force Base, FL.

Qian, S. and V. C. Li. 2011. Headed Anchor/Engineered Cementitious Composites (ECC) Pullout Behavior. *Journal of Advanced Concrete Technology*, Vol. 9, No. 3, pp. 339–351.

Rangan, B. V. 2008. *Fly Ash-Based Geopolymer Concrete*. Curtin University of Technology, Perth, Australia.

Sarker, P. K. 2011. Bond Strength of Reinforcing Steel Embedded in Fly Ash-Based Geopolymer Concrete. *Materials and Structures*, Vol. 44, No. 5, pp. 1021–1030.

Sarker, P. K., R. Haque, and K. V. Ramgolam. 2013. Fracture Behavior of Heat Cured Fly-ash-based Geopolymer Concrete. *Materials & Design*, Vol. 44, pp. 580–586.

Skvara, F., P. Svoboda, J. Dolezal, L. Kopecky, S. Pawlasova, L. Myskova, M. Lucuk, K. Dvoracek, M. Beksa, and R. Sulc. 2006. Concrete Based on Fly Ash Geopolymers. Paper presented at the Tenth East Asia-Pacific Conference on Structural Engineering and Construction, August 3–5, Bangkok, Thailand.

Sofi, M., J. S. J. van Deventer, P. A. Mendis, and G. C. Lukey. 2007. Engineering Properties of Inorganic Polymer Concretes (IPCs). *Cement and Concrete Research*, Vol. 37, No. 2, pp. 251–257.

Song, S., D. Sohn, H. M. Jennings, and T. O. Mason. 2000. Hydration of Alkali-Activated Ground Granulated Blast Furnace Slag. *Journal of Materials Science*, Vol. 35, No. 1, pp. 249–257.

Sumajouw, D. M. J., D. Hardjito, S. E. Wallah, and B. V. Rangan. 2004. Geopolymer Concrete for a Sustainable Future. Paper presented at the 2nd International Conference on the Sustainable Processing of Minerals, Green Processing, May 10–12, Fremantle, Australia.

Temuujin, J., A. van Riessen, and K. J. D. MacKenzie. 2010. Preparation and Characterisation of Fly Ash Based Geopolymer Mortars. *Construction and Building Materials*, Vol. 24, No. 10, pp. 1906–1910.

Wardhono, A., D. W. Law, Sutikno, and H. Dani. 2017. The Effect of Slag Addition on Strength Development of Class C Fly Ash Geopolymer Concrete at Normal Temperature. *American Institute of Physics (AIP) Conference Proceedings*, Vol. 1887, No. 1, pp. 020030-1–020030-7.

Wang, K. and Z. Ge. 2003. *Evaluating Properties of Blended Cements for Concrete Pavements*. National Concrete Pavement Technology (CP Tech) Center (previously Center for Portland Cement Concrete Pavement Technology), Iowa State University, Ames, IA.

Xie, Z. and Y. Xi. 2001. Hardening Mechanisms of an Alkaline-Activated Class F Fly Ash. *Cement and Concrete Research*, Vol. 31, No. 9, pp. 1245–1249.

Zivica, V., M. T. Palou, and M. Krizma. 2014. Geopolymer Cements and Their Properties: A Review. *Building Research Journal*, Vol. 61, No. 2, pp. 85–100.

Zuda, L., Z. Pavlik, P. Rovnanikova, P. Bayer, and R. Cerny. 2006. Properties of Alkali Activated Aluminosilicate Material after Thermal Load. *International Journal of Thermophysics*, Vol. 27, No. 4, pp. 1250–1263.

THE INSTITUTE FOR TRANSPORTATION IS THE FOCAL POINT FOR TRANSPORTATION AT IOWA STATE UNIVERSITY.

InTrans centers and programs perform transportation research and provide technology transfer services for government agencies and private companies;

InTrans manages its own education program for transportation students and provides K-12 resources; and

InTrans conducts local, regional, and national transportation services and continuing education programs.

IOWA STATE UNIVERSITY

Visit www.InTrans.iastate.edu for color pdfs of this and other research reports.